The Sixteenth Marcel Grossmann Meeting Downloaded from www.worldscientific.com
by GERMAN ELECTRON SYNCHROTRON @ HAMBURG on 01/30/23. Re-use and distribution is strictly not permitted, except for Open Access articles.

Absorption of massless scalar waves by electrically charged regular black holes

Marco A. A. de Paula[1,*], Luiz C. S. Leite[1,2,†], and Luís C. B. Crispino[1,‡]

[1] *Programa de Pós-Graduação em Física, Universidade Federal do Pará, 66075-110, Belém, Pará, Brazil*

[2] *Campus Altamira, Instituto Federal do Pará, 68377-630, Altamira, Pará, Brazil*

[*] *E-mail: marco.paula@icen.ufpa.br*

[†] *E-mail: luiz.leite@ifpa.edu.br*

[‡] *E-mail: crispino@ufpa.br*

We study the absorption cross section of a massless test scalar field, for arbitrary frequency values, in the background of an Ayón-Beato-García electrically charged regular black hole spacetime. We show that Ayón-Beato-García regular black holes can mimic the absorption properties of Reissner-Nordström black holes in the whole frequency range, for small-to-moderate values of the normalized electric charge.

Keywords: Regular black holes; scalar field; absorption cross section.

1. Introduction

General relativity (GR) is a geometric theory of gravity that over more than one hundred years has successfully passed several experimental tests.[1–3] The observational evidences of GR[4–6] confirm the existence of black holes (BHs). These objects are characterized by a one-way membrane, called the event horizon, and in standard GR they are normally associated to a curvature singularity. Since the known laws of physics break down at such singularities, the standard GR is not able to explain the physics of a BH singular core.

An attempt to avoid the curvature singularity issues are the so-called regular BH (RBH) spacetimes,[7] i.e., singularity-free black hole geometries. The first exact charged RBH solution was proposed in 1998 by Eloy Ayón-Beato and Alberto García (ABG).[8] This solution was based on the minimal coupling between gravity and a nonlinear electrodynamics model, and describes a static and electrically charged RBH. The nonlinear electrodynamics theory can be seen as a possible generalization of Maxwell's linear electrodynamics for strong electromagnetic fields.[9]

In real astrophysical scenarios BHs are surrounded by distributions of matter.[10] Among the bosonic and fermionic distributions of matter, the simplest one is the scalar field, corresponding to spinless particles.[11] It is possible to study how BHs absorb and scatter matter fields as an attempt to better comprehend how BHs interact with their surroundings.[12–17] We present a selection of results for the massless scalar absorption by ABG RBHs, focusing in the possibility of RBHs mimic the absorption properties of standard BHs. More details on this work are presented in a previously published paper (see Ref. 18).

The Sixteenth Marcel Grossmann Meeting Downloaded from www.worldscientific.com
by GERMAN ELECTRON SYNCHROTRON @ HAMBURG on 01/30/23. Re-use and distribution is strictly not permitted, except for Open Access articles.

2. Ayón-Beato-García RBH Spacetime

The line element of the ABG solution is given by[8]

$$ds^2 = f(r)dt^2 - f(r)^{-1}dr^2 - r^2\left(d\theta^2 + \sin^2\theta\, d\varphi^2\right), \tag{1}$$

with

$$f(r) = f^{\rm ABG}(r) \equiv 1 - \frac{2Mr^2}{(r^2+Q^2)^{3/2}} + \frac{Q^2r^2}{(r^2+Q^2)^2}, \tag{2}$$

where M and Q are the mass and the electric charge of the BH, respectively. The asymptotic limits of the metric function are given by

$$\lim_{r\to 0} f^{\rm ABG}(r) \approx \ f^{\text{de Sitter}}(r) = 1 - \frac{1}{3}\left[\frac{3\left(2|Q|M - Q^2\right)}{Q^4}\right] r^2 \tag{3}$$

and

$$\lim_{r\to\infty} f^{\rm ABG}(r) \approx \ f^{\rm RN}(r) = 1 - \frac{2M}{r} + \frac{Q^2}{r^2}. \tag{4}$$

The ABG solution describes RBHs when $|Q| \leq Q_{\rm ext} \approx 0.6341M$. For $|Q| < Q_{\rm ext}$ we have a Cauchy, r_-, and an event horizon, r_+, given by

$$r_\pm = |Q|\sqrt{\left(\pm\frac{\sqrt{-\frac{9(12s^2-1)}{\sqrt{u(s)}} - 12s^2 - \frac{u(s)}{6} + \frac{9}{2}}}{2\sqrt{6}s} + \frac{\sqrt{u(s)}}{12s} + \frac{1}{4s}\right)^2 - 1}, \tag{5}$$

where $s \equiv |Q|/(2M)$ and

$$u(s) \equiv 6\left(-\frac{4(11s^2-3)s}{\sqrt[3]{g(s)}} + s\sqrt[3]{g(s)} - 4s^2 + \frac{3}{2}\right), \tag{6}$$

$$g(s) \equiv 4(74s^3 + 3\sqrt{3}\sqrt{400s^6 - 112s^4 + 47s^2 - 4} + 9s). \tag{7}$$

On the other hand, $Q = Q_{\rm ext}$ corresponds to the so-called extreme ABG RBH, for which we have only one horizon; while $Q > Q_{\rm ext}$ corresponds to a horizonless solution. The regularity of the solution at the core of the geometry is evidenced by the behavior of the scalar invariants presented in Ref. 8, which are all regular there.

3. Absorption of Massless Test Scalar Fields

3.1. *Massless scalar field*

The massless and chargeless test scalar field Φ obeys the Klein-Gordon equation:

$$\nabla_\mu\nabla^\mu\Phi = \frac{1}{\sqrt{-g}}\partial_\mu\left(\sqrt{-g}g^{\mu\nu}\partial_\nu\right)\Phi = 0. \tag{8}$$

The Sixteenth Marcel Grossmann Meeting Downloaded from www.worldscientific.com by GERMAN ELECTRON SYNCHROTRON @ HAMBURG on 01/30/23. Re-use and distribution is strictly not permitted, except for Open Access articles.

We can decompose Φ as

$$\Phi = \sum C_{\omega l} \left(\frac{\psi_{\omega l}(r)}{r} P_l(\cos\theta) e^{-i\omega t} \right), \tag{9}$$

where $C_{\omega l}$ are constant coefficients. The indexes ω and l denote the frequency and the angular momentum of the wave, respectively, $\psi_{\omega l}(r)$ is the radial function and P_l are the Legendre Polynomials.

By inserting Eq. (9) into Eq. (8) we may find the following radial equation

$$\frac{d^2}{dr_\star^2}\psi_{\omega l} + \left[\omega^2 - V_{\rm eff}(r)\right]\psi_{\omega l} = 0, \tag{10}$$

where $\frac{dr_\star}{dr} \equiv \frac{1}{f(r)}$ is the tortoise coordinate and the effective potential $V_{\rm eff}(r)$ reads

$$V_{\rm eff}(r) \equiv f(r)\left[\frac{1}{r}\frac{df(r)}{dr} + \frac{l(l+1)}{r^2}\right]. \tag{11}$$

In Fig. 1 we present the effective potential in the background of ABG RBHs. We note that the peak of the effective potential increases as we consider higher values of the normalized charge $\alpha \equiv Q/Q_{\rm ext}$, as well as higher values of l; and for the asymptotic limits, we have $\lim_{r_\star \to \pm\infty} V_{\rm eff}(r_\star) = 0$.

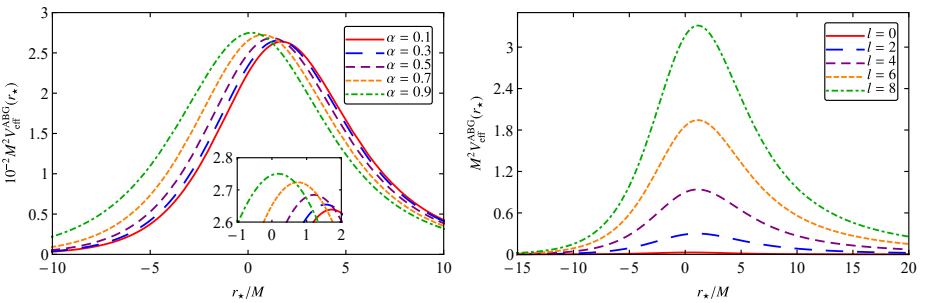

Fig. 1. The effective potential of scalar waves in the background of the ABG RBH, as a function of $r_\star$: (i) with $l = 0$, for different choices of the normalized charge α (left panel); and (ii) for different choices of l, with $\alpha = 0.8$ (right panel). The lower inset in the left panel emphasizes the peaks of the effective potential.

The appropriate boundary conditions are given by plane waves incoming from the infinite null past (the so-called *in modes*), so that the solutions of Eq. (10) reads

$$\psi_{\omega l} \sim \begin{cases} T_{\omega l} e^{-i\omega r_\star}, & r \to r_+ \ (r_\star \to -\infty), \\ e^{-i\omega r_\star} + R_{\omega l} e^{i\omega r_\star}, & r \to \infty \ (r_\star \to \infty), \end{cases} \tag{12}$$

where $T_{\omega l}$ and $R_{\omega l}$ are complex coefficients. By using the conservation of the flux, one can show that the transmission $|T_{\omega l}|^2$ and reflection $|R_{\omega l}|^2$ coefficients satisfy

$$|R_{\omega l}|^2 + |T_{\omega l}|^2 = 1. \tag{13}$$

The Sixteenth Marcel Grossmann Meeting Downloaded from www.worldscientific.com
by GERMAN ELECTRON SYNCHROTRON @ HAMBURG on 01/30/23. Re-use and distribution is strictly not permitted, except for Open Access articles.

3.2. *Absorption cross section*

By using the so-called partial-wave method, we may write the total absorption cross section (ACS) of the massless scalar wave as a sum of partial-waves contributions, given by[19]

$$\sigma = \sum_{l=0}^{\infty} \sigma_l, \tag{14}$$

where the partial ACS, σ_l, reads

$$\sigma_l = \frac{\pi}{\omega^2}(2l+1)|T_{\omega l}|^2. \tag{15}$$

There are analytic approximations for the ACS of massless test scalar fields by BHs in the low- and high-frequency regimes. In the low-frequency regime, for stationary BH geometries, the ACS tends to the surface area of the BH event horizon, namely[20,21]

$$\mathrm{A} = 4\pi r_+^2. \tag{16}$$

On the other hand, in the high-frequency regime, the absorption of a massless scalar field is governed by the geometric cross section (GCS) of null geodesics, i.e., $\sigma_{\rm gcs} = \pi b_c^2$, where b_c is the critical impact parameter. By using the so-called sinc approximation, it is possible to obtain an improvement for the high-frequency approximation, which can be expressed as[22]

$$\sigma_{\rm hf} = \sigma_{\rm gcs}\left[1 - 8\pi b_c \Lambda e^{-\pi b_c \Lambda}\mathrm{sinc}\left(2\pi b_c \omega\right)\right], \tag{17}$$

where $\mathrm{sinc}(x) \equiv \sin(x)/x$, and Λ is the Lyapunov exponent.[23]

4. Results

4.1. *Main features*

The numerical method employed to obtain the ACS consists in integrating numerically Eq. (10) from very close to the BH event horizon r_+, up to some radial position very far from the BH, with the boundary conditions in these regions given by Eq. (12).

In Fig. 2 we show the total ACS, normalized by the BH area, for distinct ABG RBHs. We note that, as $\omega \to 0$, the ratio σ/A tends to the unity. Hence, at the low-frequency limit, the numerical result for the ACS tends to the BH area, as expected.

A comparison between the horizon area of ABG and RN BHs is presented in Fig. 3. We see that for fixed values of α, ABG and RN BHs have very similar BH areas.

In Fig. 4 we compare the total ACS obtained numerically with the analytic approximations for the high-frequency regime (see Subsec. 3.2). As we can see, in this frequency regime, the total ACS obtained numerically oscillates around the

The Sixteenth Marcel Grossmann Meeting Downloaded from www.worldscientific.com
by GERMAN ELECTRON SYNCHROTRON @ HAMBURG on 01/30/23. Re-use and distribution is strictly not permitted, except for Open Access articles.

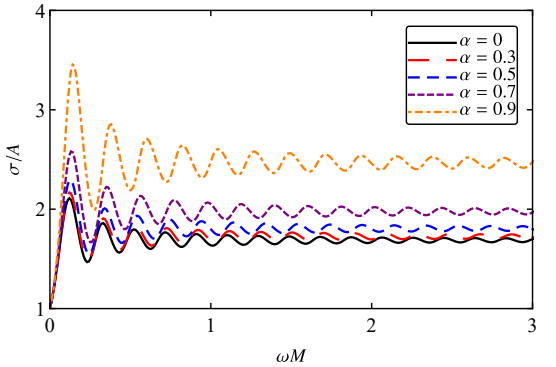

Fig. 2. The total ACS of the scalar wave for distinct ABG RBHs (divided by the BH area), as a function of ωM. We also exhibit, for comparison, the results for the Schwarzschild case ($\alpha = 0$).

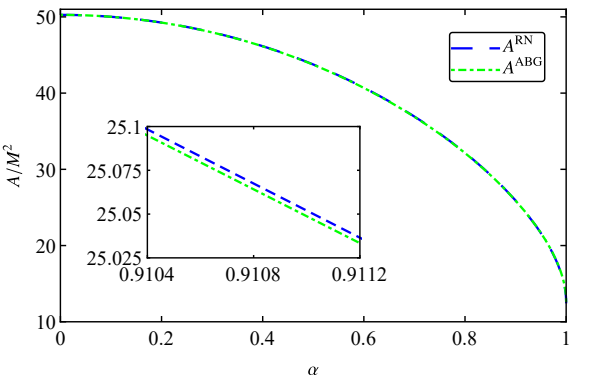

Fig. 3. The surface area of the BH event horizon of ABG and RN BHs, as a function of the normalized charge. The central inset shows the areas of ABG and RN BHs for α between 0.9104 and 0.9116, emphasizing the high similarity between the corresponding areas.

corresponding GCS and the oscillatory profile is very well reproduced by the sinc approximation. These results, combined with the ones for the low-frequency regime (cf. Fig. 2), show that our numerical results are consistent with the analytic approximations available in the literature. We also see that the total ACS of the ABG RBH diminishes as we increase α, so that the wave is more absorbed in the background of small-charge ABG RBH spacetimes. This is in accordance with the fact that the potential barrier raises as we increase α (see Fig. 1).

Examples of partial ACSs in the background of different ABG RBHs are shown in Fig. 5. We observe that the peak of the partial-wave modes diminishes as we consider higher values of the normalized electric charge and the mode $l = 0$ provides the main contributions for the ACS in the low-frequency regime.

The Sixteenth Marcel Grossmann Meeting Downloaded from www.worldscientific.com
by GERMAN ELECTRON SYNCHROTRON @ HAMBURG on 01/30/23. Re-use and distribution is strictly not permitted, except for Open Access articles.

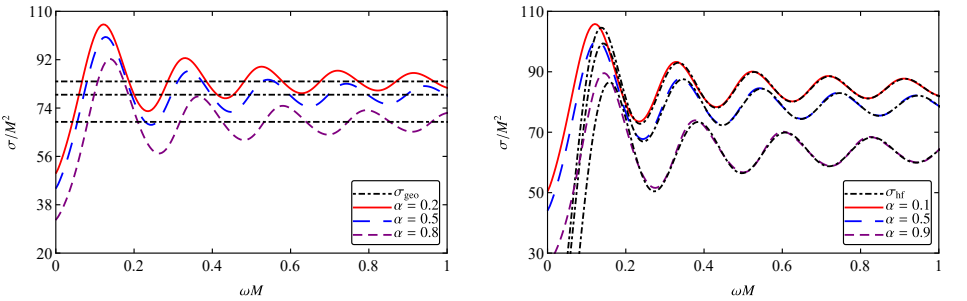

Fig. 4. Comparison of the total ACS (as a function of ωM) of the ABG RBH obtained numerically with: (i) the corresponding GCSs (left panel) and (ii) the corresponding sinc approximation (right panel), considering distinct values of α.

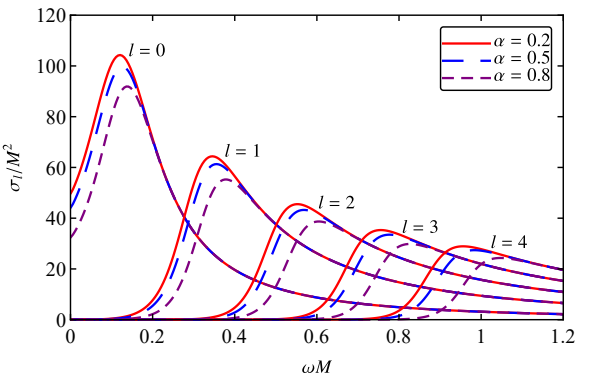

Fig. 5. Partial ACSs of the scalar wave considering different ABG RBHs (distinct values of α), as functions of ωM.

In Fig. 6 we compare the absorption results for ABG and RN BHs, considering two values of α. The total ACS of the ABG RBH is typically larger than the corresponding RN case. However, for small values of α, the total ACS of ABG and RN BH solutions can be very similar for arbitrary values of the frequency. Notice also that the zero-frequency regime of the total ACSs of ABG and RN BHs are very similar, for the same α value. This is in agreement with the behavior of their areas which are very similar for the same choices of α (cf. Fig. 3).

4.2. *RBHs as standard BHs mimickers*

We can consider the values of $(\alpha^{\rm ABG}, \alpha^{\rm RN})$ for which the corresponding GCSs coincide in order to find situations in which the absorption results of ABG and RN BHs are very similar. In Fig. 7 we display such values, which can be found up to $(\alpha^{\rm ABG}, \alpha^{\rm RN}) = (1, 0.9161)$.

The Sixteenth Marcel Grossmann Meeting Downloaded from www.worldscientific.com
by GERMAN ELECTRON SYNCHROTRON @ HAMBURG on 01/30/23. Re-use and distribution is strictly not permitted, except for Open Access articles.

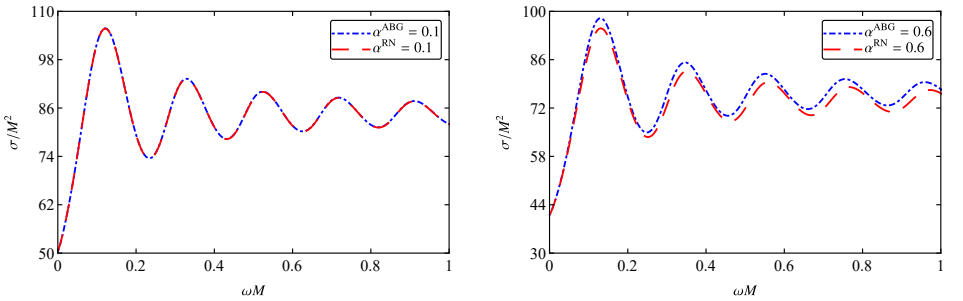

Fig. 6. The total ACSs of ABG and RN BHs as a function of ωM, for $\alpha = 0.1$ (left panel) and for $\alpha = 0.6$ (right panel).

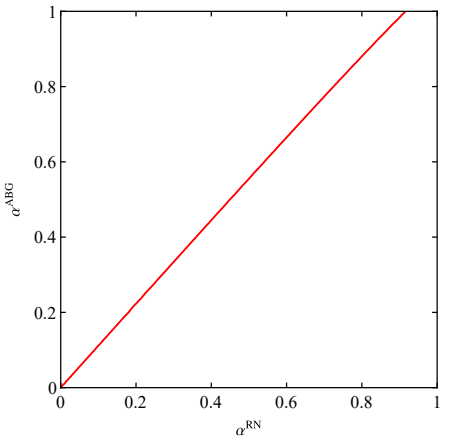

Fig. 7. The values of the normalized charges for which the GCSs of ABG and RN BHs coincide.

In Fig. 8 we exhibit the total ACSs for two pairs of $(\alpha^{\rm ABG}, \alpha^{\rm RN})$, for which the GCSs coincide. For low-to-moderate α values, the total ACSs of the ABG and RN BHs are basically indistinguishable along the whole frequency regime. This contrasts with the absorption results for massless test scalar fields in the Bardeen case,[24] for which the ACSs of Bardeen and RN BH solutions can be very similar only in the high-frequency regime.

We can define a function to estimate the percentual deviation between the BH area of each pair $(\alpha^{\rm ABG}, \alpha^{\rm RN})$, namely

$$\mathrm{A}_{\rm dif} \equiv \frac{\mathrm{A}^{\rm RN} - \mathrm{A}^{\rm ABG}}{\mathrm{A}^{\rm ABG}} 100\%. \tag{18}$$

The smaller the function $\mathrm{A}_{\rm dif}$ is, the more similar are the ABG and RN BHs areas. In Table 1 we present the corresponding BH areas, as well as $\mathrm{A}_{\rm dif}$, for several pairs $(\alpha^{\rm ABG}, \alpha^{\rm RN})$ displayed in Fig. 7. As we can see, the function $\mathrm{A}_{\rm dif}$ increases with

The Sixteenth Marcel Grossmann Meeting Downloaded from www.worldscientific.com
by GERMAN ELECTRON SYNCHROTRON @ HAMBURG on 01/30/23. Re-use and distribution is strictly not permitted, except for Open Access articles.

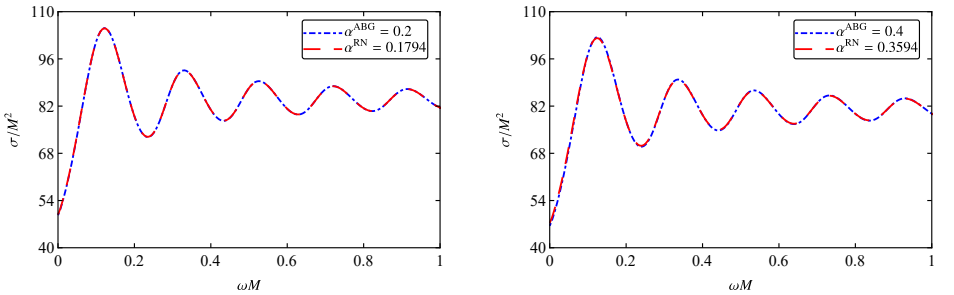

Fig. 8. The total ACS for the pairs $(\alpha^{\rm ABG}, \alpha^{\rm RN}) = (0.2, 0.1794)$ (left panel) and $(\alpha^{\rm ABG}, \alpha^{\rm RN}) = (0.4, 0.3594)$ (right panel). In both cases, the corresponding GCSs coincide.

Table 1. The BH areas and $\rm A_{dif}$ for several pairs $(\alpha^{\rm ABG}, \alpha^{\rm RN})$ shown in Fig. 7.

$\alpha^{\rm ABG}$	$\alpha^{\rm RN}$	$\rm A^{ABG}/M^2$	$\rm A^{RN}/M^2$	$\rm A_{dif}$
0.1516	0.1365	49.6831	49.7961	0.2274%
0.182	0.1629	49.425	49.5963	0.3453%
0.2027	0.1815	49.2219	49.4341	0.4309%
0.2852	0.2548	48.189	48.6201	0.8946%
0.318	0.2855	47.6772	48.1951	1.0863%
0.3417	0.3054	47.2708	47.8927	1.3156%
0.4003	0.3608	46.1309	46.9368	1.7469%
0.4707	0.4226	44.4976	45.6667	2.6273%
0.5003	0.4489	43.7207	45.0586	3.0601%

the increase of α. We also note that for an ABG RBH with $\alpha \lesssim 0.5$, we have that $\rm A_{dif} \lesssim 3\%$. Therefore, pairs $(\alpha^{\rm ABG}, \alpha^{\rm RN})$ that satisfy $\sigma^{\rm ABG}_{\rm gcs} = \sigma^{\rm RN}_{\rm gcs}$ correspond to very similar BH areas, as long as we consider only low-to-moderate values of α, implying that the ACSs of ABG and RN BHs are very similar also at the low-frequency regime. This also contrasts with the absorption results for massless test scalar field in the Bardeen case.[24]

5. Final Remarks

We revisited the scalar absorption of massless scalar fields by the first electrically charged ABG RBH solution,[18] presenting a selection of additional results. The height of potential barrier (related to the propagation of massless scalar waves in the background of the ABG RBH) enhances as we increase l or α. The ACSs obtained with our numerical method tend to the corresponding BH area in the low-frequency regime, as expected,[20] and, in this limit, the mode $l = 0$ provides the

The Sixteenth Marcel Grossmann Meeting Downloaded from www.worldscientific.com
by GERMAN ELECTRON SYNCHROTRON @ HAMBURG on 01/30/23. Re-use and distribution is strictly not permitted, except for Open Access articles.

main contribution to the ACS. We also obtained that the BH areas of ABG and RN BHs are very similar for certain values of α.

The total ACS of the ABG RBH, in the mid-to-high frequency limit, oscillates around the corresponding GCS and the sinc approximation provides excellent results for ACS in this regime. Therefore, considering the results in the low- and high-frequency regime, we conclude that our numerical results for the ACS agree very well with the analytic approximations. We also noted that the ABG RBH total ACS diminishes as we increase α, what is in accordance with the fact that $V_{\text{eff}}(r)$ increases as we increase α. The ABG RBH total ACS is typically larger than the RN one, for the same choice of α, but it is possible to find situations for which the total ACSs of ABG and RN BHs are very similar in the whole frequency range, mainly for small values of α. This similarity shows that it is possible that electrically charged RBHs mimic standard BHs, in what concerns the absorption of massless test scalar fields.

Acknowledgments

We are grateful to Conselho Nacional de Desenvolvimento Científico e Tecnológico (CNPq) and Coordenação de Aperfeiçoamento de Pessoal de Nível Superior (CAPES) – Finance Code 001, from Brazil, for partial financial support. This research has also received funding from the European Union's Horizon 2020 research and innovation programme under the H2020-MSCA-RISE-2017 Grant No. FunFiCO-777740.

References

1. C. M. Will, The Confrontation between General Relativity and Experiment, Living Rev. Relativ. **17**, 4 (2014).
2. L. C. B. Crispino and D. J. Kennefick, A hundred years of the first experimental test of general relativity, Nat. Phys. **115**, 416 (2019).
3. L. C. B. Crispino and S. Paolantonio, The first attempts to measure light deflection by the Sun, Nat. Astron. **4**, 6 (2020).
4. R. Narayan and J. E. McClintock, Observational Evidence for Black Holes, arXiv:1312.6698 [astro-ph.HE].
5. B. P. Abbott *et al.* [LIGO Scientific Collaboration and Virgo Collaboration], Observation of Gravitational Waves from a Binary Black Hole Merger, Phys. Rev. Lett. **116**, 061102 (2016).
6. The Event Horizon Telescope Collaboration *et al.*, First M87 Event Horizon Telescope Results. I. The Shadow of the Supermassive Black Hole, Atrophys. J. **875**, L1 (2019).
7. J. Bardeen, Non-singular General Relativistic Gravitational Collapse, in *Proceedings of the International Conference GR5* (Tbilisi, Georgia, U.S.S.R., 1968), p. 174.
8. E. Ayón-Beato and A. García, Regular Black Hole in General Relativity Coupled to Nonlinear Electrodynamics, Phys. Rev. Lett. **80**, 5056 (1998).
9. M. Born and L. Infeld, Foundations of the new field theory, Proc. R. Soc. A **144**, 425 (1934).
10. R. Narayan, Black holes in astrophysics, New J. Phys. **7**, 199 (2005).

The Sixteenth Marcel Grossmann Meeting Downloaded from www.worldscientific.com
by GERMAN ELECTRON SYNCHROTRON @ HAMBURG on 01/30/23. Re-use and distribution is strictly not permitted, except for Open Access articles.

11. W. Greiner and J. Reinhardt, *Field Quantization* (Springer, Berlim, 1996).
12. J. A. Futterman, F. A. Handler, and R. A. Matzner, *Scattering from Black Holes* (Cambridge University Press, Cambridge, England, 1988).
13. L. C. B. Crispino, S. R. Dolan, and E. S. Oliveira, Scattering of massless scalar waves by Reissner-Nordström black holes, Phys. Rev. D **79**, 0640022 (2009).
14. E. S. Oliveira, L. C. B. Crispino, and A. Higuchi, Equality between gravitational and electromagnetic absorption cross sections of extreme Reissner-Nordstrom black holes, Phys. Rev. D **84**, 084048 (2011).
15. L. C. B. Crispino, S. R. Dolan, A. Higuchi, and E. S. de Oliveira, Inferring black hole charge from backscattered electromagnetic radiation, Phys. Rev. D **90**, 064027 (2014).
16. L. C. B. Crispino, S. R. Dolan, A. Higuchi, and E. S. de Oliveira, Scattering from charged black holes and supergravity, Phys. Rev. D **92**, 084056 (2015).
17. C. L. Benone and L. C. B. Crispino, Superradiance in static black hole spacetimes, Phys. Rev. D **93**, 024028 (2016).
18. M. A. A. Paula, L. C. S. Leite, and L. C. B. Crispino, Electrically charged black holes in linear and non-linear electrodynamics: Geodesic analysis and scalar absorption, Phys. Rev. D **102**, 104033 (2020).
19. W. Unruh, Absorption cross section of small black holes, Phys. Rev. D **14**, 3251 (1976).
20. S. R. Das, G. Gibbons, and S. D. Mathur, Universality of Low Energy Absorption Cross Sections for Black Holes, Phys. Rev. Lett. **78**, 417 (1997).
21. A. Higuchi, Low-frequency Scalar absorption cross sections for stationary black holes, Classical Quantum Gravity **18**, L139 (2001); **19**, 599(A) (2002).
22. Y. Décanini, G. Esposito-Farèse, and A. Folacci, Universality of high-energy absorption cross sections for black holes, Phys. Rev. D **83**, 044032 (2011).
23. V. Cardoso, A. S. Miranda, E. Berti, H. Witek, and V. T. Zanchin, Geodesic stability, Lyapunov exponents, and quasinormal modes, Phys. Rev. D **79**, 064016 (2009).
24. C. F. B. Macedo and L. C. B. Crispino, Absorption of planar massless scalar waves by Bardeen regular black holes, Phys. Rev. D **90**, 064001 (2014).